Mu-7, a New Layered Aluminophosphate $[CH_3NH_3]_3[Al_3P_4O_{16}]$ with a 4 × 8 Network: Characterization, Structure, and Possible Crystallization Mechanism

L. Vidal,[†] C. Marichal,[†] V. Gramlich,[‡] J. Patarin,*[,†] and Z. Gabelica[†]

Laboratoire de Matériaux Minéraux, ENSCMu, Université de Haute Alsace, UPRES-A 7016, 3 rue Alfred Werner, 68093 Mulhouse Cedex, France, and Laboratorium für Kristallographie, ETH-Zentrum, CH-8092 Zürich, Switzerland

Received March 1, 1999. Revised Manuscript Received July 12, 1999

The title compound, Mu-7, is a new layered aluminophosphate. It was obtained from a quasi-nonaqueous system involving methylformamide (MF) as solvent in addition to restricted amounts of water. MF is decomposed into methylamine during synthesis and the latter is occluded into the interlayer spacing of the material. The structure was determined by single-crystal X-ray diffraction. The symmetry is triclinic, space group $P\bar{1}$, $a = 8.368(7)$, $b = 11.274(10)$, $c = 11.462(12)$ Å, $\alpha = 72.40(7)$, $\beta = 89.45(8)$, and $\gamma = 85.37(7)°$. Mu-7 is built from zigzag ladder-type chains connected to form layers containing only four- and eight-membered rings. Mu-7 is the first lamellar aluminophosphate having such a 4 × 8 network. Characterization of the new compound by ^{13}C, ^{27}Al, and ^{31}P solid-state NMR spectroscopy, bulk chemical analysis and TG/DSC is reported. A possible crystallization mechanism based on the condensation between "parent" ($[AlP_2O_8H_2]^-$) and zigzag ladder-type ($[Al_4P_4O_{20}H_4]^{4-}$) chains is proposed.

Introduction

In 1982, Wilson et al.[1] reported the existence of a new generation of molecular sieves based on an aluminophosphate framework and named $AlPO_4$-*n*. They usually contain alternating tetrahedrally coordinated AlO_4 and PO_4 units. Some members of the $AlPO_4$-*n* family have structures analogous to those of zeolites. For instance, $AlPO_4$-GIS[2] and $AlPO_4$-20[3] are isostructural with gismondine and sodalite, respectively. Other compounds such as VPI-5[4] or JDF-20[5] do not have zeolite counterparts.

The crystallization mechanisms of aluminophosphates have been widely debated in the literature but most of them still remain unclear. Nevertheless, their crystallization was recently claimed to proceed through the initial formation of mono- and bidimensional anionic species.[6,7] In a first step, a "parent" chain ($[AlP_2O_8H_2]^-$) would crystallize. Further hydrolysis and condensation reactions of this linear chain would lead to the formation of more complex chain structures. By following the same hydrolysis−condensation process, lamellar and finally three-dimensional frameworks could be obtained.

Layered aluminophosphate compounds consist of continuous anionic aluminophosphate sheets regularly stacked along with interlamellar positively charged organic species. To our knowledge, these compounds involve layers consisting only of 4 × 6, 4 × 6 × 8, 4 × 6 × 12, and 8 × 8 networks and have the following established compositions: $[Al_3P_4O_{16}]^{3-}$, $[Al_2P_3O_{12}H_x]^{(3-x)-}$ ($x = 1-2$),[7] $[AlP_2O_8]$,[3−8,9] $[Al(HPO_4)_2(H_2O)_2]^-$,[10] and $[Al_4P_5O_{20}H]^{2-}$.[11]

In the past decade, numerous layered aluminophosphates have been obtained under hydrothermal[8,9,12−20]

[†] Université de Haute Alsace.
[‡] ETH-Zentrum.

(1) Wilson, S. T.; Lok, B. M.; Messina, C. A.; Cannan, T. R.; Flanigen, E. M. *J. Am. Chem. Soc.* **1982**, *101*, 1146.
(2) Paillaud, J. L.; Marler, B.; Kessler, H. *J. Chem. Soc., Chem. Commun.* **1996**, 1293.
(3) Wilson, S. T.; Lok, B. M.; Flanigen, E. M. U.S. Patent 4 310 440, 1982.
(4) Davis, M. E.; Montes, C.; Garces, J. M. In *Zeolite Synthesis*; Occelli, M. L., et al., Eds.; American Chemical Society: Washington D.C. 1991; p 291.
(5) Huo, Q.; Xu, R.; Li, S.; Ma, Z.; Thomas, J. M.; Chippindale, A. M. *J. Chem. Soc., Chem. Commun.* **1992**, 929.
(6) Oliver, S.; Kuperman, A.; Lough, A.; Ozin, G. A. *Chem. Mater.* **1996**, *8*, 2391.
(7) Oliver, S.; Kuperman, A.; Ozin, G. A. *Angew. Chem., Int. Engl. Ed.* **1998**, *37*, 46.
(8) Tielli, W.; Long, Y.; Pang, W. *J. Solid State Chem.* **1990**, *89*, 392.
(9) Morgan, K. R.; Gainsford, G. J.; Milestone, N. B. *J. Chem. Soc., Chem. Commun.* **1997**, 61.
(10) Leech, M. A.; Cowley, A. R.; Prout, K.; Chippindale, A. M. *Chem. Mater.* **1998**, *10*, 451.
(11) Vidal, L.; Gramlich, V.; Patarin, J.; Gabelica, Z. *Eur. J. Solid State Inorg. Chem.* **1996**, *35*, 545.
(12) Kraushaar-Czarnetzki, B.; Stork, W. H. J.; Dogterom, R. *J. Inorg. Chem.* **1993**, *32*, 5029.
(13) Bruce, D. A.; Wilkinson, A. P.; White, M. G.; Bertrand, J. A. *J. Chem. Soc., Chem. Commun.* **1995**, 2059.
(14) Morgan, K. R.; Gainsford, G. J.; Milestone, N. B. *J. Chem. Soc., Chem. Commun.* **1995**, 425.
(15) Bontchev, R. P.; Sevov, S. C. *Chem. Mater.* **1997**, *9*, 3155.
(16) Gray, M. J.; Jasper, J. D.; Wilkinson, A. P.; Hausen, J. C. *Chem. Mater.* **1997**, *9*, 976.
(17) Thomas, J. M.; Jones, R. H.; Xu, R.; Chen, J.; Chippindale, A. M.; Natarajan, S.; Cheetham, A. K. *J. Chem. Soc., Chem. Commun.* **1992**, 929.
(18) Jones, R. H.; Chippindale, A. M.; Natarajan, S.; Thomas, J. M. *J. Chem. Soc., Chem. Commun.* **1994**, 565.

10.1021/cm991027o CCC: $18.00
Published on Web 09/18/1999

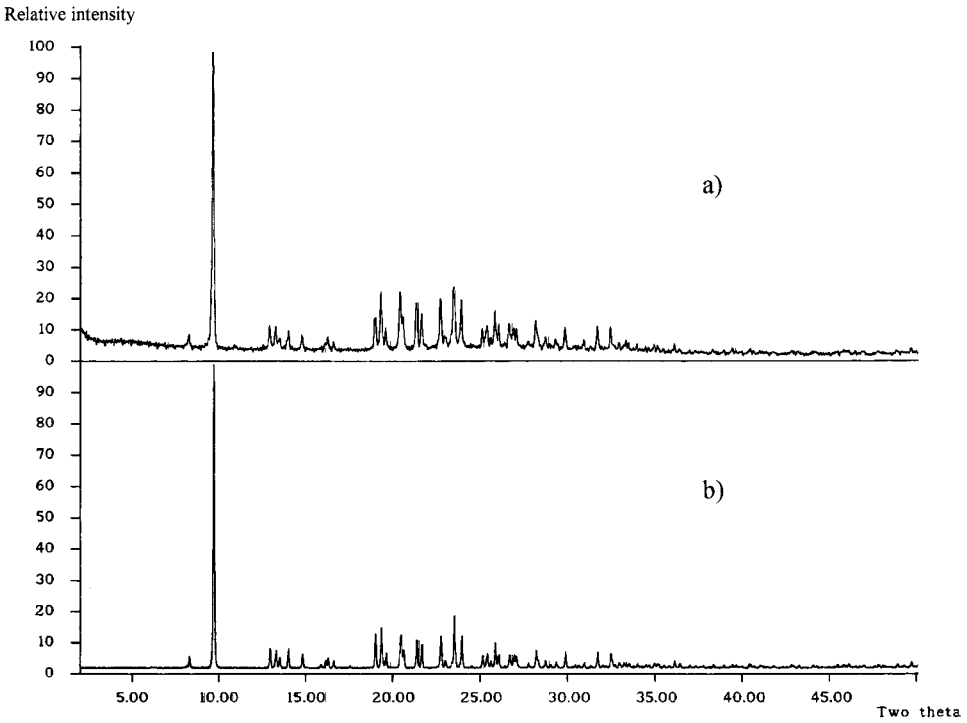

Figure 1. Powder XRD pattern (Cu $K\alpha_1$) of the as-synthesized aluminophosphate Mu-7: (a) experimental and (b) calculated from the structure data.

or solvothermal conditions.[8,9,11,21−29] In aqueous media, their nucleation and growth are so fast that the detection and characterization of the aluminophosphate precursors is difficult. Replacing partly or quasi-totally water by an organic solvent was shown to dramatically change the whole chemistry of such synthesis mixtures.[30] However, some water, even in small proportions, was shown to be necessary for crystallization to occur.[7,30] The kinetics of hydrolysis and condensation reactions was nevertheless sufficiently decreased so that various new layered aluminophosphates could be obtained.[8,9,11,21−29] Organic solvents having both a high dielectric constant and a high dipolar moment so as to favor the dissociation and the solvation of the various species present in the reaction mixture can partly replace water. Various mono- and dialkylformamides involve such properties. Dimethylformamide (DMF) and diethylformamide (DEF) were the only solvents used so far in addition to water for the synthesis of $AlPO_4$ compounds. A monoclinic variant of the sodalite-type aluminophosphate[31] and a GIS-type aluminophosphate[2] were obtained in the presence of DMF, whereas a new layered aluminophosphate (Mu-4)[11] crystallized in the presence of DEF.

Table 1. Recording Conditions for the MAS and CP-MAS NMR Spectra

	^{13}C	^{31}P	^{27}Al
chemical shift reference	$Si(CH_3)_4$	85 wt % H_3PO_4	$Al(H_2O)_6^{3+}$
technique (probe)	CPMAS (4 mm)	MAS (2.5 mm)	MAS (4 mm)
frequency (MHz)	75.47	161.98	104.26
pulse width (μs) (corresponding flip angle)	6.5 (90°)	3 (90°)	0.7 (15°)
contact time (ms)	1	/	/
recycle time (s)	4	360	1
spinning rate (kHz)	4	29	12
no. of scans	195	2	22

In the present work, we report the synthesis, the full characterization, and the crystal structure of a new layered aluminophosphate, $[CH_3NH_3]_3[Al_3P_4O_{16}]$ named Mu-7 (Mu standing for Mulhouse).[32] Mu-7 was obtained from a quasi-nonaqueous reaction mixture involving methylformamide (MF) as the main solvent. A possible crystallization mechanism is also proposed.

Experimental Section

Synthesis. Mu-7 was prepared from a gel containing alumina and orthophosphoric acid as reactants and methylformamide as the main solvent. The water content stems from the aluminum and phosphorus sources. Typically, 1.40 g of pseudo-boehmite (Condéa, hydrated alumina, water loss at 600

(19) Barrett, P. A.; Jones, R. H. *J. Chem. Soc., Chem. Commun.* **1995**, 1979.
(20) Cheng, S.; Tzeng, J. N.; Hsu, B. Y. *Chem. Mater.* **1997**, *9*, 1788.
(21) Chippindale, A. M.; Powell, A. V.; Bull, L. M.; Jones, R. H.; Cheetham, A. K.; Thomas, J. M.; Xu, R. *J. Solid State Chem.* **1992**, *96*, 199.
(22) Chippindale, A. M.; Natarajan, S.; Thomas, J. M.; Jones, R. H. *J. Solid State Chem.* **1994**, *111*, 18.
(23) Chippindale, A. M.; Huo, Q.; Jones, R. H.; Thomas, J. M.; Walton, R.; Xu, R. *Stud. Surf. Sci. Catal.* **1995**, *98*, 26.
(24) Oliver, S.; Kuperman, A.; Lough, A.; Ozin, G. A. *Inorg. Chem.* **1996**, *35*, 6373.
(25) Oliver, S.; Kuperman, A.; Lough, A.; Ozin, G. A. *J. Chem. Soc., Chem. Commun.* **1996**, 1761.
(26) Oliver, S.; Kuperman, A.; Lough, A.; Ozin, G. A. *J. Mater. Chem.* **1997**, *7*, 807.
(27) Chippindale, A. M.; Cowley, A. R.; Huo, Q.; Jones, R. H.; Law, A. D.; Thomas, J. M.; Xu, R. *J. Chem. Soc., Dalton Trans.* **1997**, 2639.
(28) Gao, Q.; Chen, J.; Xu, R.; Yue, Y. *Chem. Mater.* **1997**, *9*, 457.
(29) Gao, Q.; Li, B.; Chen, J.; Williams, I. D.; Zheng, J.; Barber, D. *J. Solid State Chem.* **1997**, *129*, 37.
(30) Oliver, S.; Kuperman, A.; Lough, A.; Ozin, G. A.; Garces, J. M.; Olken, M. M.; Rudlof, P. *Stud. Surf. Sci. Catal.* **1994**, *84*, 219.
(31) Vidal, L.; Paillaud, J. L.; Gabelica, Z. *Microporous Mesoporous Mater.* **1998**, *24*, 189.
(32) Vidal L.; Gramlich V.; Patarin J.; Gabelica Z. *Chem. Lett.* **1999**, *2*, 201.

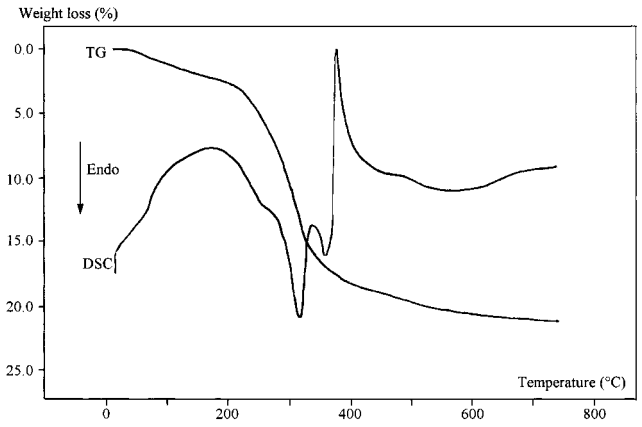

Figure 2. TG/DSC curves under air of the as-synthesized aluminophosphate Mu-7.

Table 2. Summary of the Experimental and Crystallographic Data for $[CH_3NH_3]_3[Al_3P_4O_{16}]$

chemical formula	$[CH_3NH_3]_3[Al_3P_4O_{16}]$
crystal system	triclinic
space group	$P\bar{1}$
a (Å)	8.368(7)
b (Å)	11.274(10)
c (Å)	11.462(12)
α (deg)	72.40(7)
β (deg)	89.45(8)
γ (deg)	85.35(7)
V (Å^3); Z	1027(2); 2
M; ρ calcd	557.02; 1.801
radiation; λ (Å)	Cu Kα; 1.54178
crystal size (μm)	100 × 100 × 20
diffractometer	Picker STOE DIF4
collection method	$\omega - 2\theta$
adsorption coefficient (mm^{-1})	5.421
adsorption correction	unapplied
reflection collected	2114
independent reflections	2114
refinement method	full-matrix least-squares on F^2
data/restraint/parameters	2113/0/269
(hkl) min; (hkl) max	−8−10 0; 8 11 11
2 θ max (deg)	50
final R indices [$I > 2\sigma(I)$]	R1 = 0.0372 wR2 = 0.0873
R indices (all data)	R1 = 0.0698 wR2 = 0.0988
largest difference peak and hole	0.367 and −0.360 e Å^{-3}

°C, 24.4 wt %) were added to 8.0 g of methylformamide (Fluka, analytical grade). The suspension was stirred until homogeneity. Orthophosphoric acid (3.21 g, Fluka, 85 wt % H_3PO_4 in water) was further added to the mixture. The final suspension was stirred for a few minutes until it cooled to room temperature. The final gel had the following molar composition: 0.75 Al_2O_3:1.0 P_2O_5:3.3 H_2O:10.0 MF. The gel was then heated in a Teflon-lined stainless steel autoclave (20 cm^3) at 170 °C under autogenous pressure for 7 days. The crystalline product was filtered, washed with distilled water, and dried at 60 °C overnight.

Characterization. The as-synthesized product was characterized by powder X-ray diffraction (XRD) (STOE STADI-P diffractometer using Cu Kα radiation with a curved germanium-(111) primary monochromator and a linear position-sensitive detector). Scanning electron microscopy (SEM) (Philips XL30 microscope) was used to determine the crystal morphology and size. The amounts of Al, P, C, and N in the as-synthesized product were determined by chemical bulk analysis (Centre d'Analyse du CNRS, Solaize, France) using inductively coupled plasma emission spectroscopy for Al and P and coulometry and catharometry for C and N after calcination of the sample. The amounts of organic species and water occluded within the structure of Mu-7 were determined by combined thermogravimetry (TG) and differential scanning calorimetry (DSC) (Setaram TG/DSC 111 thermoanalyzer). The as-synthesized product was heated from room temperature to 750 °C at a rate of 5 °C min^{-1} under air flow.

Table 3. Atomic Coordinates and Equivalent Isotropic Displacement Parameters for $[CH_3NH_3]_3[Al_3P_4O_{16}]$[a]

atom	x	y	z	U_{eq} (Å^2)
P(1)	0.4766(2)	0.1934(1)	0.0197(1)	0.014(1)
P(2)	0.0226(2)	0.1056(1)	−0.2396(1)	0.015(1)
P(3)	0.0216(2)	0.5283(1)	−0.3139(1)	0.013(1)
P(4)	0.5258(2)	0.2325(1)	−0.3807(1)	0.015(1)
Al(5)	−0.1485(2)	0.3475(2)	−0.4257(2)	0.015(1)
Al(6)	0.6803(2)	0.0507(2)	−0.1324(2)	0.014(1)
Al(7)	0.2606(2)	0.2887(2)	−0.2161(2)	0.014(1)
O(8)	0.5408(4)	0.2670(3)	0.0939(3)	0.022(1)
O(9)	0.3897(4)	0.2783(3)	−0.0964(3)	0.020(1)
O(10)	0.5789(5)	0.1205(4)	−0.2708(3)	0.025(1)
O(11)	−0.0391(5)	0.2070(3)	−0.3570(3)	0.024(1)
O(12)	0.3679(4)	0.2926(4)	−0.3490(3)	0.023(1)
O(13)	−0.1179(4)	0.0715(4)	−0.1521(3)	0.024(1)
O(14)	0.1429(4)	0.1631(3)	−0.1772(3)	0.022(1)
O(15)	0.0972(5)	−0.0061(3)	−0.2695(4)	0.024(1)
O(16)	0.1443(5)	0.4273(3)	−0.2394(4)	0.025(1)
O(17)	0.6496(4)	0.3291(4)	−0.4016(4)	0.025(1)
O(18)	−0.1031(5)	0.4645(4)	−0.3665(4)	0.028(1)
O(19)	0.5060(4)	0.1906(4)	−0.4913(3)	0.022(1)
O(20)	−0.0557(4)	0.6025(3)	−0.2390(3)	0.023(1)
O(21)	0.6124(4)	0.1144(3)	−0.0198(3)	0.022(1)
O(22)	0.3536(4)	0.1061(3)	0.0926(3)	0.020(1)
O(29)	0.1120(5)	0.6122(4)	−0.4203(3)	0.030(1)
N(1)	0.2907(6)	0.0102(5)	0.5357(5)	0.037(2)
N(2)	0.3901(6)	0.3494(4)	0.2683(5)	0.029(1)
N(3)	0.8731(6)	0.2565(4)	0.1344(4)	0.024(1)
C(1)	0.1908(9)	0.0690(8)	0.4254(7)	0.053(2)
C(2)	0.4658(9)	0.4672(7)	0.2425(9)	0.062(3)
C(3)	0.9495(9)	0.2877(8)	0.0143(6)	0.055(2)

[a] Standard deviations are in parentheses.

Table 4. Atomic Coordinates for Hydrogen Atoms and Isotropic Displacement Parameters for $[CH_3NH_3]_3[Al_3P_4O_{16}]$[a]

atom	x	y	z	U_{eq}(Å^2)
H(31)	0.8903(37)	0.1749(7)	0.1718(15)	0.036
H(32)	0.7681(8)	0.2772(31)	0.1246(5)	0.036
H(33)	0.9145(32)	0.2985(26)	0.1797(13)	0.036
H(21)	0.4292(33)	0.3073(17)	0.2186(24)	0.044
H(22)	0.2846(8)	0.3654(5)	0.2563(33)	0.044
H(23)	0.4105(38)	0.3040(16)	0.3457(11)	0.044
H(3D)	0.9288(50)	0.3754(11)	−0.0267(20)	0.082
H(3E)	0.9065(44)	0.2411(35)	−0.0339(18)	0.082
H(3F)	1.0631(12)	0.2671(44)	0.0251(7)	0.082
H(2D)	0.4390(52)	0.5181(21)	0.1604(18)	0.093
H(2E)	0.5801(10)	0.4501(7)	0.2512(48)	0.093
H(2F)	0.4279(50)	0.5106(25)	0.2990(32)	0.093
H(1A)	0.1162(39)	0.0119(18)	0.4164(25)	0.079
H(1B)	0.2580(10)	0.0899(41)	0.3549(9)	0.079
H(1C)	0.1332(44)	0.1434(25)	0.4328(20)	0.079
H(11)	0.3340(41)	−0.0637(18)	0.5334(19)	0.055
H(12)	0.2304(12)	0.0001(36)	0.6019(5)	0.055
H(13)	0.3682(31)	0.0589(19)	0.5388(21)	0.055

[a] Standard deviations are in parentheses. All hydrogen atoms were placed with geometrical constraints.

^{13}C CP-MAS NMR spectroscopy was used to determine the nature of the organic species occluded into the structure. ^{27}Al and ^{31}P MAS NMR spectroscopies were used to characterize the short-range atomic arrangement in the as-synthesized material. The spectra were recorded on a Bruker DSX 400 spectrometer (^{27}Al, ^{31}P) and on Bruker MSL300 spectrometer (^{13}C). The recording conditions for the CP-MAS and MAS NMR spectra are given in Table 1. The two-dimensional ^{27}Al 3Q-MAS spectrum was recorded on a Bruker DSX400 spectrometer using a 2.5 mm Bruker MAS probe. A z-filtered MQMAS pulse sequence was used.[33] The triple quantum coherence was excited with a 2.5 μs pulse (ν_{rf} = 227 kHz). The spinning speed

Table 5. Bond Lengths (Å) for $[CH_3NH_3]_3[Al_3P_4O_{16}]$[a]

P(1)−O(8)	1.486(4)	Al(5)−O(17)$^{\#2}$	1.728(4)
P(1)−O(9)	1.534(4)	Al(5)−O(11)	1.730(4)
P(1)−O(21)	1.536(4)	Al(6)−O(13)$^{\#3}$	1.727(4)
P(1)−O(22)	1.542(4)	Al(6)−O(21)	1.728(4)
P(2)−O(15)	1.490(4)	Al(6)−O(22)$^{\#4}$	1.733(4)
P(2)−O(14)	1.532(4)	Al(6)−O(10)	1.737(5)
P(2)−O(13)	1.534(4)	Al(7)−O(16)	1.722(4)
P(2)−O(11)	1.539(4)	Al(7)−O(9)	1.724(4)
P(3)−O(20)	1.480(4)	Al(7)−O(14)	1.735(4)
P(3)−O(16)	1.522(4)	Al(7)−O(12)	1.751(4)
P(3)−O(29)	1.535(4)	O(13)−Al(6)$^{\#2}$	1.727(4)
P(3)−O(18)	1.538(4)	O(17)−Al(5)$^{\#3}$	1.728(4)
P(4)−O(19)	1.496(4)	O(22)−Al(6)$^{\#4}$	1.733(4)
P(4)−O(12)	1.527(4)	O(29)−Al(5)$^{\#1}$	1.716(5)
P(4)−O(10)	1.528(4)	N(3)−C(3)	1.467(8)
P(4)−O(17)	1.529(4)	N(2)−C(2)	1.466(8)
Al(5)−O(29)$^{\#1}$	1.716(5)	N(1)−C(1)	1.470(9)
Al(5)−O(18)	1.724(4)		

[a] Symmetry transformations used to generate equivalent atoms: #1: $-x, -y+1, -z-1$; #2: $x-1, y, z$; #3: $x+1, y, z$; #4: $-x+1, -y, -z$.

Table 6. Bond angles (deg) for $[CH_3NH_3]_3[Al_3P_4O_{16}]$

O(8)−P(1)-O(9)	111.5(2)	O(29)$^{\#1}$−Al(5)−O(11)	107.6(2)
O(8)−P(1)-O(21)	110.9(2)	O(18)−Al(5)-O(11)	112.9(2)
O(9)−P(1)-O(21)	107.8(2)	O(17)$^{\#2}$−Al(5)−O(11)	109.4(2)
O(8)−P(1)-O(22)	110.9(2)	O(13)$^{\#3}$−Al(6)−O(21)	108.2(2)
O(9)−P(1)-O(22)	106.7(2)	O(13)$^{\#3}$−Al(6)−O(22)$^{\#4}$	111.2(2)
O(21)−P(1)-O(22)	108.8(2)	O(21)−Al(6)-O(22)$^{\#4}$	110.5(2)
O(15)−P(2)-O(14)	111.6(2)	O(13)$^{\#3}$−Al(6)−O(10)	109.3(2)
O(15)−P(2)-O(13)	111.2(2)	O(21)−Al(6)-O(10)	112.0(2)
O(14)−P(2)-O(13)	107.1(2)	O(22)$^{\#4}$−Al(6)−O(10)	105.7(2)
O(15)−P(2)-O(11)	110.5(2)	O(16)−Al(7)-O(9)	105.9(2)
O(14)−P(2)-O(11)	107.4(2)	O(16)−Al(7)-O(14)	110.8(2)
O(13)−P(2)-O(11)	108.8(2)	O(9)−Al(7)-O(14)	109.8(2)
O(20)−P(3)-O(16)	111.7(2)	O(16)−Al(7)-O(12)	109.3(2)
O(20)−P(3)-O(29)	110.4(2)	O(9)−Al(7)-O(12)	110.6(2)
O(16)−P(3)-O(29)	106.8(2)	O(14)−Al(7)-O(12)	110.3(2)
O(20)−P(3)-O(18)	111.2(2)	P(1)−O(9)-Al(7)	146.8(2)
O(16)−P(3)-O(18)	108.0(2)	P(4)−O(10)-Al(6)	153.0(3)
O(29)−P(3)-O(18)	108.7(2)	P(2)−O(11)-Al(5)	149.4(3)
O(19)−P(4)-O(12)	110.9(2)	P(4)−O(12)-Al(7)	136.8(3)
O(19)−P(4)-O(10)	109.9(2)	P(2)−O(13)-Al(6)$^{\#2}$	148.5(3)
O(12)−P(4)-O(10)	108.0(2)	P(2)−O(14)-Al(7)	138.1(3)
O(19)−P(4)-O(17)	111.3(2)	P(3)−O(16)-Al(7)	151.4(3)
O(12)−P(4)-O(17)	107.5(2)	P(4)−O(17)-Al(5)$^{\#3}$	142.5(3)
O(10)−P(4)-O(17)	109.1(2)	P(3)−O(18)-Al(5)	149.5(3)
O(29)$^{\#1}$−Al(5)−O(18)	110.8(2)	P(1)−O(21)-Al(6)	145.7(3)
O(29)$^{\#1}$−Al(5)−O(17)$^{\#2}$	109.4(2)	P(1)−O(22)-Al(6)$^{\#4}$	138.3(2)
O(18)−Al(5)-O(17)#2	106.8(2)	P(3)−O(29)-Al(5)$^{\#1}$	145.8(3)

[a] Symmetry transformations used to generate equivalent atoms: #1: $-x, -y+1, -z-1$; #2: $x-1, y, z$; #3: $x+1, y, z$; #4: $-x+1, -y, -z$.

was adjusted to 10 kHz, the acquisition being rotor-synchronized.

Results and Discussion

Powder X-ray Diffraction. The new aluminophosphate only crystallizes when water is present as reactant in the reaction mixture. Indeed, using dehydrated alumina and anhydrous orthophosphoric acid as Al and P sources respectively, only traces of Mu-7 were obtained, an unidentified compound cocrystallizing as the major product.

A typical XRD pattern of Mu-7 is reported in Figure 1a. This diffractogram fits well the symmetry and the cell parameters determined from the single-crystal structure analysis, as compared with the calculated pattern (STOE software package) (Figure 1b).

Table 7. Anisotropic Displacement Parameters ($Å^2 \times 10^3$) for $[CH_3NH_3]_3[Al_3P_4O_{16}]$[a]

atom	U_{11}	U_{22}	U_{33}	U_{23}	U_{13}	U_{12}
P(1)	14(1)	12(1)	14(1)	−3(1)	2(1)	−3(1)
P(2)	10(1)	16(1)	20(1)	−4(1)	5(1)	−5(1)
P(3)	12(1)	13(1)	13(1)	−3(1)	3(1)	−3(1)
P(4)	11(1)	19(1)	14(1)	−4(1)	3(1)	−7(1)
Al(5)	13(1)	16(1)	15(1)	−4(1)	3(1)	−8(1)
Al(6)	11(1)	14(1)	16(1)	−2(1)	4(1)	−5(1)
Al(7)	9(1)	17(1)	15(1)	−2(1)	3(1)	−4(1)
O(8)	15(2)	29(2)	27(2)	−16(2)	2(2)	−2(2)
O(9)	19(2)	15(2)	22(2)	0(2)	−3(2)	−6(2)
O(10)	27(2)	22(2)	20(2)	3(2)	−1(2)	0(2)
O(11)	25(2)	21(2)	21(2)	1(2)	2(2)	0(2)
O(12)	16(2)	29(3)	21(2)	−3(2)	5(2)	0(2)
O(13)	13(2)	31(3)	27(2)	−6(2)	10(2)	−13(2)
O(14)	19(2)	24(2)	24(2)	−7(2)	6(2)	−12(2)
O(15)	23(2)	17(2)	32(3)	−9(2)	9(2)	0(2)
O(16)	22(2)	21(2)	28(2)	−3(2)	−1(2)	5(2)
O(17)	15(2)	24(2)	38(3)	−10(2)	7(2)	−12(2)
O(18)	19(2)	32(3)	38(3)	−18(2)	0(2)	−8(2)
O(19)	23(2)	27(2)	19(2)	−11(2)	2(2)	−8(2)
O(20)	20(2)	26(2)	30(3)	−17(2)	1(2)	−5(2)
O(21)	20(2)	21(2)	25(2)	−7(2)	2(2)	−3(2)
O(22)	18(2)	15(2)	26(2)	−2(2)	12(2)	−8(2)
O(29)	42(3)	30(3)	15(2)	3(2)	7(2)	−22(2)
N(1)	33(3)	41(4)	47(4)	−26(3)	24(3)	−18(3)
N(2)	25(3)	31(3)	29(3)	−6(3)	4(3)	1(2)
N(3)	19(3)	23(3)	33(3)	−11(2)	5(2)	−7(2)
C(1)	46(5)	69(6)	52(5)	−31(5)	5(4)	−10(4)
C(2)	48(5)	42(5)	113(7)	−45(5)	37(5)	−25(4)
C(3)	46(5)	90(7)	37(5)	−29(5)	17(4)	−20(5)

[a] The anisotropic displacement factor takes the form $-2\pi^2[h^2a^{*2}U_{11}+...0.2hka^*b^*U_{12}]$.

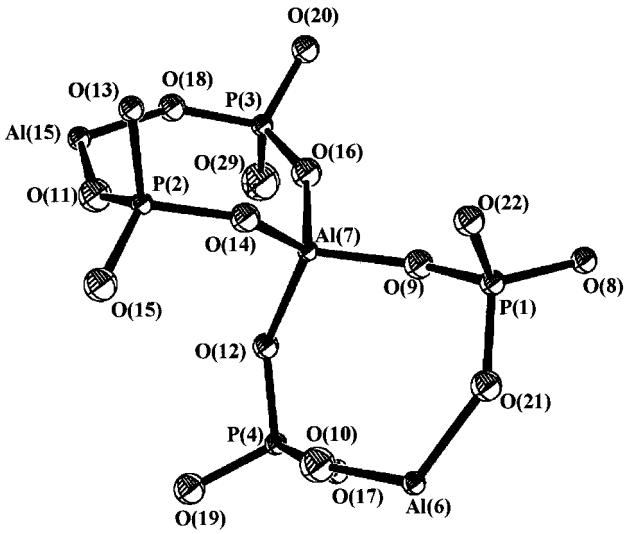

Figure 3. Asymmetric structural unit of Mu-7.

Crystal Morphology and Chemical and Thermal Analysis. The overall morphology of Mu-7 consists of a parallel array of platelike crystals with various dimensions. Although, the thickness of most of the crystals is less than 0.5 μm, some of them proved to be appropriate for single-crystal structure determination.

The chemical formula of Mu-7, obtained from the single-crystal structure determination (see below) is $[CH_3NH_3]_3[Al_3P_4O_{16}]$. The amounts of C, N, P, and Al, as determined by chemical bulk analysis, are 6.23, 6.78, 21.43, and 15.23 wt % respectively. The Al/P molar ratio, equal to 0.80, is close to that derived from the formula

(33) Amoureux, J. P.; Fernandez, C. *Solid State NMR* **1998**, *10*, 211.

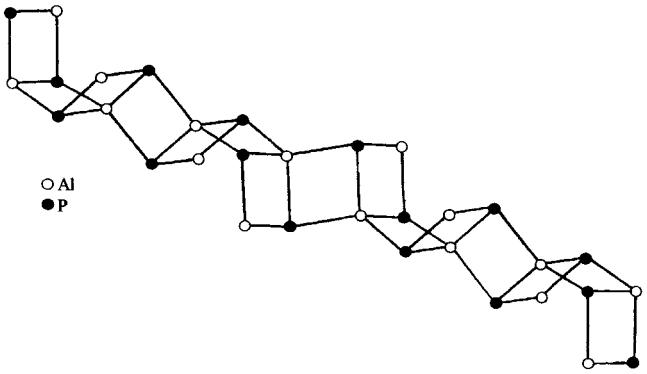

Figure 4. Section of an anionic zigzag ladder-type chain present in the Mu-7 structure. For clarity, the oxygen atoms were omitted.

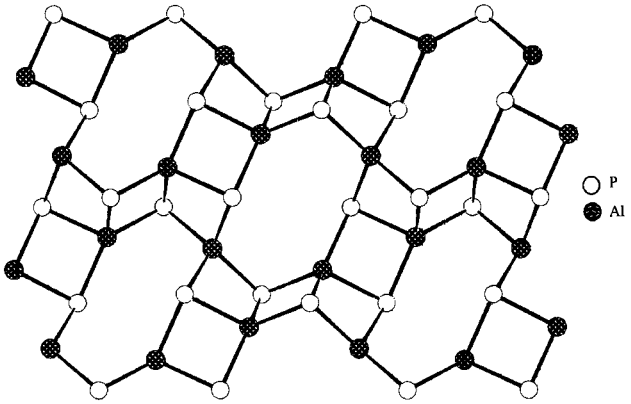

Figure 5. Projection of the structure of Mu-7 onto (011). For clarity, the oxygen and hydrogen atoms and the organic species were omitted.

(0.75). The molar ratio C/N = 1.1 shows that methylamine is occluded into the structure, instead of methylformamide (C/N = 2), suggesting that the solvent is decomposed during synthesis. Such acid-catalyzed decompositions of mono- or dialkylformamides into the corresponding amines and carbon monoxide have already been observed.[2,11] The in situ liberation of methylamine in the reaction mixture appears to be essential for the crystallization of Mu-7. Indeed, when MF is replaced by methylamine in the precursor gel, another unidentified aluminophosphate crystallizes.

Figure 2 presents the TG/DSC curves of the as-synthesized Mu-7 sample. Two distinct weight losses could be seen on the TG curves. The first one, recorded between 20 and 200 °C (∼3.0 wt %) is attributed to the elimination of physisorbed water. Nevertheless, on the basis of the structure analysis, no water was found in the as-synthesized material. Its presence might be attributed to the particular crystal morphology; indeed, residual water could be located between the aggregated platelets. The second weight loss (∼18.0 wt %), occurring between 200 and 700 °C, corresponds to the thermal decomposition of methylamine occluded into the structure. The weight loss is relatively close to the one expected (17.2 wt %) from the structure determination. The removal of the organic species is accompanied by at least one endothermic peak around 315 °C, corresponding probably to a collapse of the structure (confirmed by high-temperature XRD analysis). The endotherms were followed by an exothermic peak (380 °C),

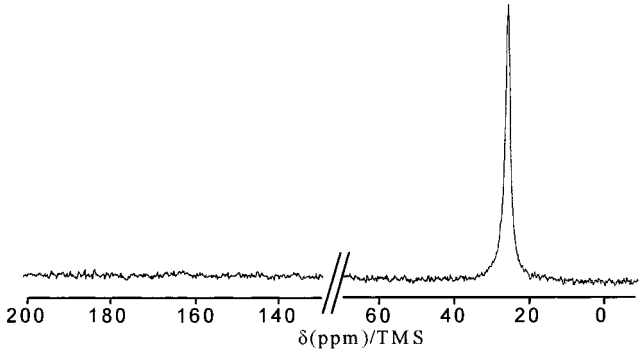

Figure 6. ^{13}C CP-MAS NMR spectrum of the as-synthesized aluminophosphate Mu-7.

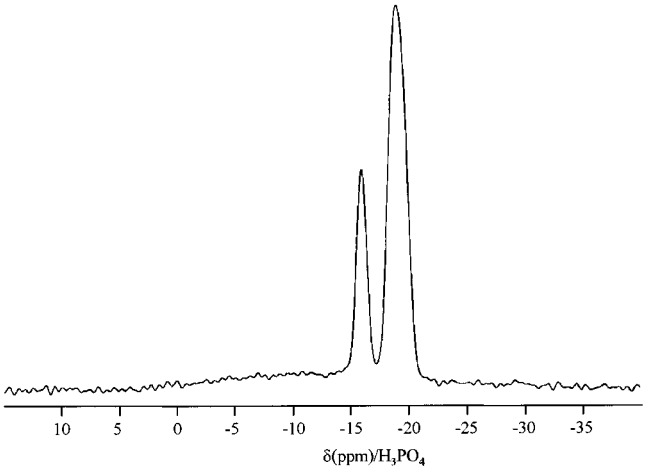

Figure 7. ^{31}P MAS NMR spectrum of the as-synthesized aluminophosphate Mu-7.

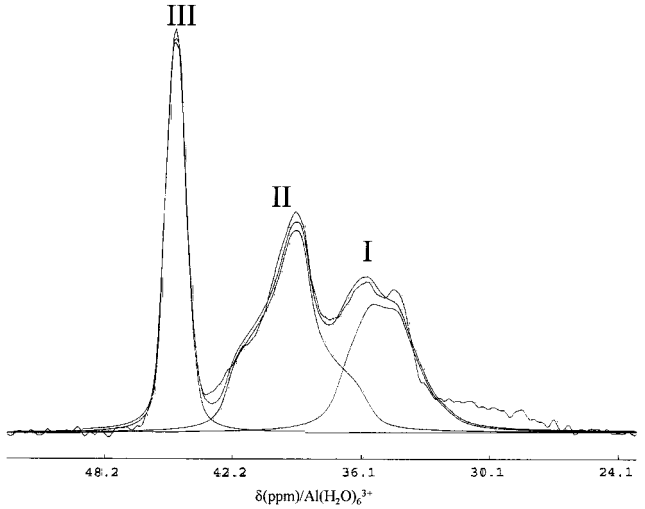

Figure 8. ^{27}Al MAS NMR spectrum of the as-synthesized aluminophosphate Mu-7 (only the isotropic region is shown).

reflecting the oxidation of the organic species. The XRD analysis performed on the residual product shows that the layered aluminophosphate is completely transformed into $AlPO_4$-type trydimite.

Crystal Structure Determination of Mu-7

Experimental. A crystal with dimensions 100 × 100 × 20 μm was selected from the batch for the structure determination. The crystal was mounted on a four-circle

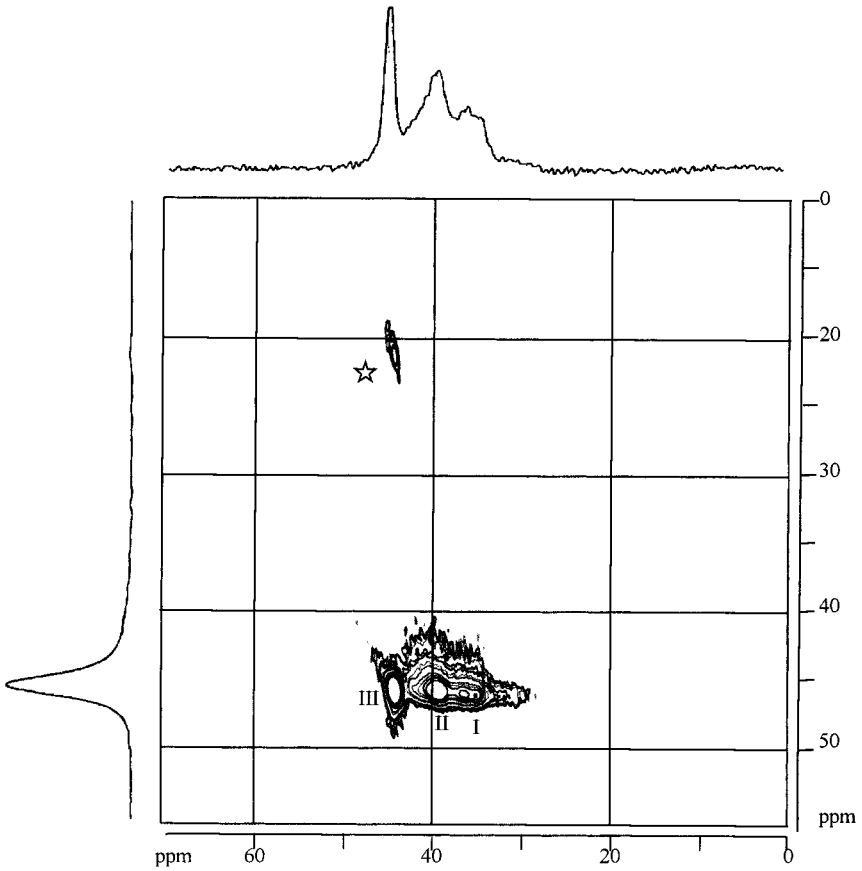

Figure 9. Sheared ^{27}Al 3Q-MAS spectrum of the as-synthesized aluminophosphate Mu-7, together with its anisotropic MAS projection on the top and triple quantum isotropic projection on the left of the 2D contour plot. (The star indicates a spinning sideband.)

Picker STOE DIF4 diffractometer. A total of 2114 reflections were recorded in ω scan mode in the θ range of 4.05−50.00° (Cu Kα radiation). The structure was solved by direct method using the SHELXS-86[34] program and refined using the SHELXL-93[35] program. A total of1541 independent reflections fulfilled the condition $I > 2\sigma I$. A summary of the experimental and crystallographic data is reported in Table 2. The atomic positions are reported in Tables 3 and 4 and bond lengths and angles in Tables 5 and 6, respectively. The hydrogen atoms of methylamine were placed with geometrical constraints. All non-hydrogen atoms were refined with anisotropic displacement parameters (Table 7) which finely led to R1 = 0.0372 ($R1 = \sum||F_0| - |F_c||/\sum|F_0|$) and wR2 = 0.0873 ($R2 = \{\sum w(F_0^2 - F_c^2)^2/\sum w(F_0^2)^2\}^{1/2}$) for 1541 reflections and R1 = 0.0698 and wR2 = 0.0988 for all data.

Structure Description. The single-crystal structure analysis reveals that Mu-7 involves a novel layer topology. Four and three distinct crystallographic sites accommodate phosphorus and aluminum atoms, respectively, which are in 4-fold coordination with oxygens. This leads to an Al/P ratio equal to 0.75. Figure 3 presents the asymmetric unit of Mu-7. Each Al shares its oxygen atoms with phosphorus neighbors with an average bong length of 1.730 Å. The P atoms are only 3-connected into the layers. The fourth P−O distance (mean P−O = 1.488 Å) probably corresponds to a phosphorus atom doubly bonded to an oxygen atom. A bond-valence calculation[36] on these oxygen atoms, taking into account the phosphorus atom and the hydrogen bonded protonated methylamine molecules (dN−H···O ≈ 1.90 Å), leads to a value close to 2. AlO_4 and PO_4 tetrahedra are linked in a strict alternation to form zigzag ladder-type chains (Figure 4). The connectivity between the chains leads to anionic $[Al_3P_4O_{16}]^{3-}$ layers, parallel to the (011) plane (Figure 5). These layers only have four- and eight-membered rings (MR). This kind of 4 × 8 network is novel for layered aluminophosphates. Indeed, only 4 × 6, 4 × 6 × 8, 4 × 6 × 12 and 8 × 8 nets were known, so far, and the 4 × 8 one was only hypothetical.[37] Methylamine, which is located in the interlayer spacing is protonated and neutralizes the negative charges of the anionic aluminophosphate layers. Moreover, as discussed above, the amine is in strong

Table 8. Quadrupolar Parameters of the Different Tetrahedral Aluminum Sites

site	I	II	III
σ_{iso} (ppm)	34	43	46
C_Q (MHz)	∼2	∼2.2	∼1
η_Q	≤0.4	≥0.8	≥0.6

(34) Scheldrick, G. M. *Program for the Resolution of Crystal Structures*; University of Göttingen: Göttingen, Germany, 1986.
(35) Scheldrick, G. M. *Program for the Resolution of Crystal Structures*; University of Göttingen: Göttingen, Germany, 1993.
(36) Brown, I. D. In *Structure and Bonding Crystals*; O'Keefe, M, Navrotsky, A., Eds.; Academic Press: New York, 1981; Vol. 2, Chapter 14.
(37) Williams, I. D.; Gao, Q.; Chen, J.; Ngai, L. Y.; Li, Z.; Xu, R. *J. Chem. Soc., Chem. Commun.* **1996**, 1781.

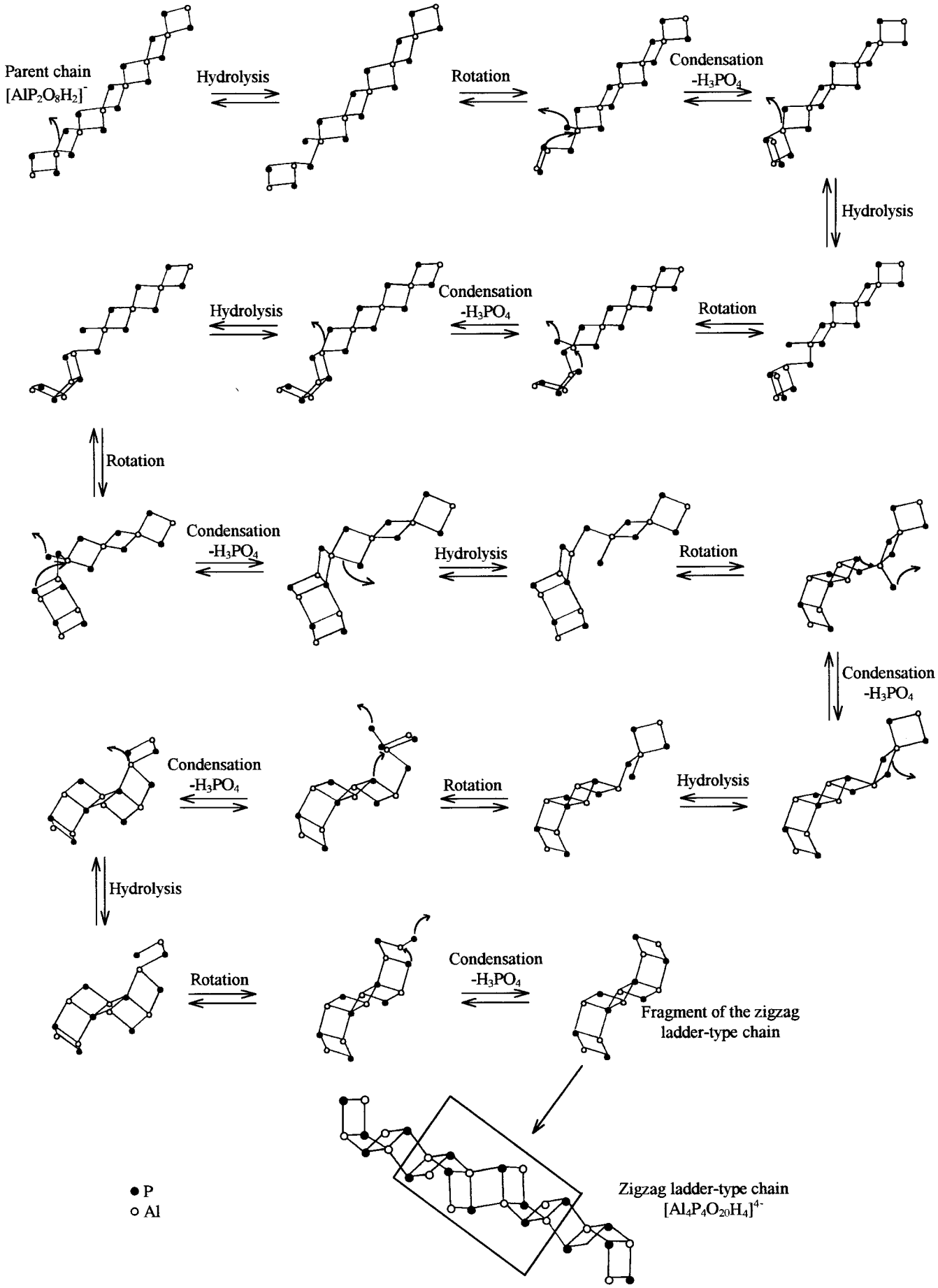

Figure 10. Possible mechanism of formation of the zigzag ladder-type chain $[Al_4P_4O_{20}H_4]^{4-}$ from the "parent" $[AlP_2O_8H_2]^-$ chain.

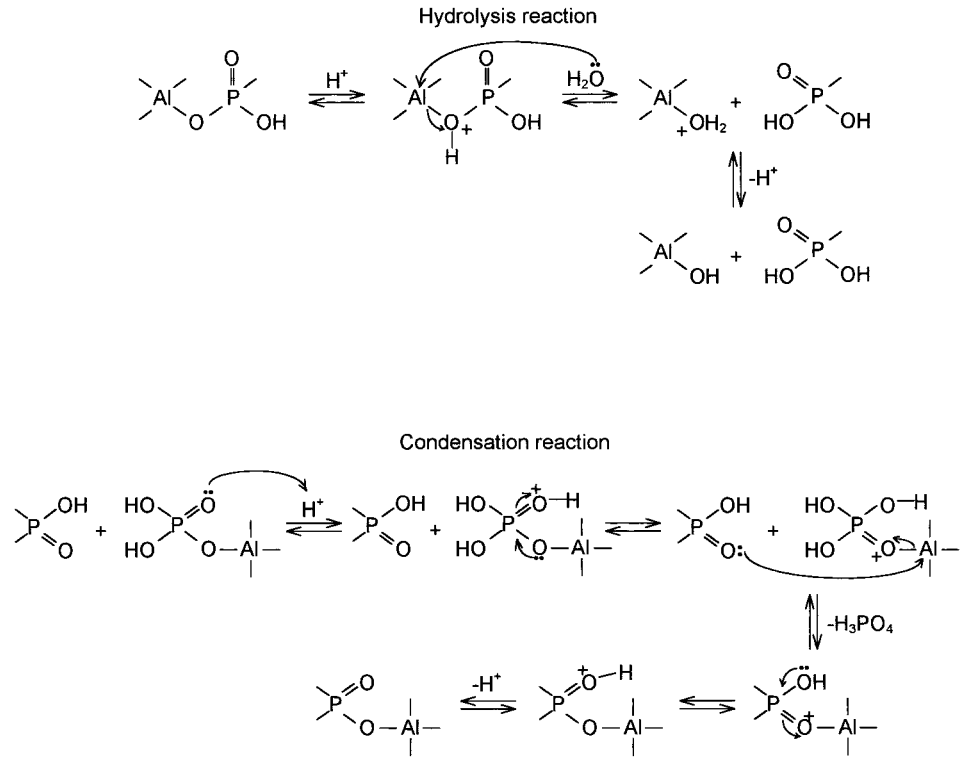

Figure 11. Hydrolysis and condensation reactions leading to the zigzag ladder-type chain $[Al_4P_4O_{20}H_4]^{4-}$.

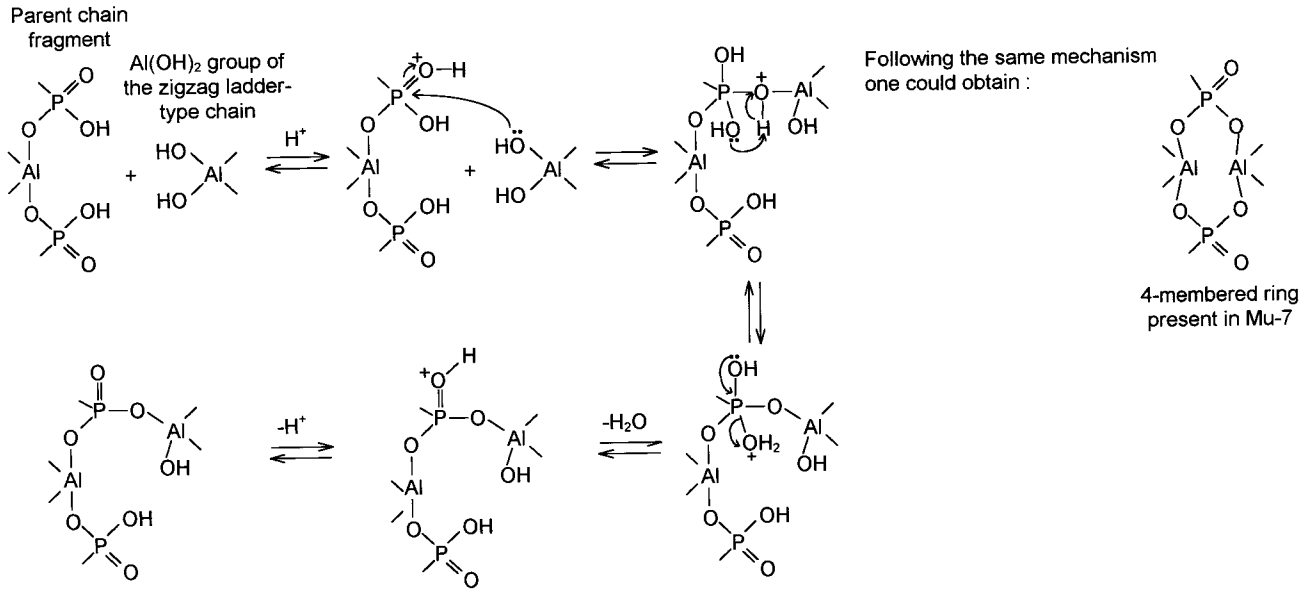

Figure 12. Condensation reactions occurring between the "parent" chain $[AlP_2O_8H_2]^-$ and the zigzag ladder-type chain $[Al_4P_4O_{20}H_4]^{4-}$.

interaction with the inorganic sheets through hydrogen bonding (dN—H···O close to 1.90 Å).

Solid-state NMR Spectroscopy

^{13}C CP-MAS NMR Spectroscopy. As shown in Figure 6, the ^{13}C CP-MAS spectrum of Mu-7 exhibits a single resonance line located at 26.2 ppm. Such a chemical shift is attributed to a N—CH_3 group.[38] No signal around 160 ppm, corresponding to a carbonyl group[38] was observed, even upon using the ^{1}H decoupled MAS technique. Such a result is in good agreement with data obtained from the single-crystal structure determination and chemical bulk and thermal analyses, which have confirmed that methylformamide was decomposed into methylamine along the crystallization process. Moreover, the chemical shift value of the methyl group at 26.2 ppm better corresponds to the protonated amine ($\delta \approx 26.3$ ppm) than to the nonprotonated amine ($\delta \approx 27.8$ ppm) (calculated with the ACD lab software).

^{31}P and ^{27}Al MAS NMR Spectroscopy. The ^{31}P MAS NMR spectrum (Figure 7) shows two main components located at −16.2 and −19.5 ppm. Their integrated intensity ratio is close to 1:3, suggesting the presence of four distinct crystallographic phosphorus sites. The three phosphorus sites, corresponding to

the component at −19.5 ppm, are probably in a very similar environment. Indeed, increasing the spinning speed up to 30 kHz did not allow the different sites to be resolved. Furthermore, a small signal recorded at −30 ppm is attributed to traces of impurities in the sample.

The ^{27}Al MAS NMR spectrum (Figure 8) presents a complex line shape in the chemical shift range of tetrahedrally coordinated aluminum.[39] Although, the MAS NMR technique can average first-order interactions, this method is not sufficient to cancel second-order quadrupolar interactions. Therefore, multiple quantum MAS NMR experiments were performed to cancel this broadening leading to high-resolution isotropic spectra.[40] The result is shown Figure 9. Despite the lack of resolution in the triple quantum isotropic projection of the 2D contour plot, the shape of the lines due to different quadrupolar parameters allowed us to separate three tetrahedral aluminum crystallographic sites, which is in agreement with the proposed structure. Numerical simulation with the Bruker Winfit software of the F2 slices yield the quadrupolar coupling constant C_Q and the asymmetry parameter η_Q for each aluminum site as given in Table 8.

Possible Crystallization Mechanism for Mu-7

As shown in the structure determination part, Mu-7 can be built from zigzag ladder-type chains. Oliver et al.[7] proposed that the crystallization of aluminophosphates proceeds through the formation of chains which would lead to more complex structures upon hydrolysis and condensation reactions. A scheme for the crystallization mechanism of Mu-7 can be described in the similar way with "parent" and zigzag ladder-type chains. The anionic "parent" chain $[AlP_2O_8H_2]^-$ consists of corner-sharing $Al_2P_2O_4$ four-rings bridged through the aluminum centers (Figure 10). Each AlO_4 tetrahedron is linked to four phosphorus atoms which are only 2-connected to the chain. They also involve one P−OH and one P═O groups. In the reaction mixture, upon hydrolysis, some of the Al−O−P bonds are broken and Al−OH and P−OH groups are formed. Rotations will bring two different P−OH groups close together and intrachain condensations will occur with a release of H_3PO_4. Depending on the reaction mixture composition, the hydrolysis−rotation−condensation process can lead to different kinds of chains. In the present case, anionic $[Al_4P_4O_{20}H_4]^{4-}$ zigzag ladder-type chains would be obtained (Figures 10 and 11). Layers of Mu-7 are formed by involving one "parent" chain and two zigzag ladder-type chains. The negative charges belonging to the two kinds of chains are neutralized by the protonated methylamine molecules. The crystallization would proceed through condensation reactions between two P−OH groups of the "parent" chain and one $Al(OH)_2$ group of the zigzag ladder-type chain, as illustrated in Figures 12 and 13.

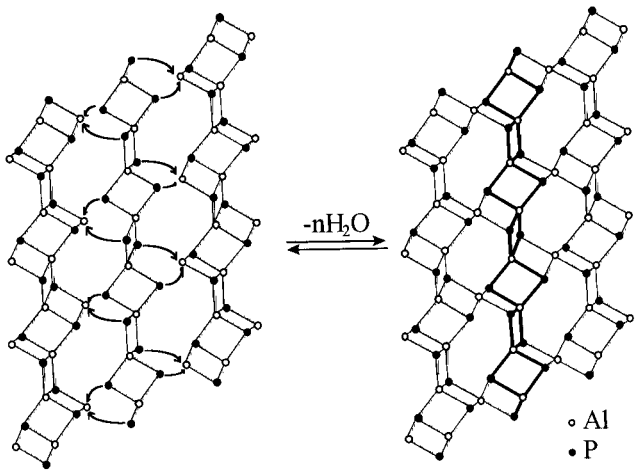

Figure 13. Possible mechanism illustrating the building of the Mu-7 layers.

The two kinds of chains involved in the building of the layers, probably very labile, could neither be isolated, nor even detected by using the above techniques. The proposed mechanism although highly likely, still requires further experimental confirmations.

Conclusion

A new layered compound Mu-7, involving a 4 × 8 aluminophosphate framework was obtained from a quasi-nonaqueous system involving methylformamide (MF) as the main solvent in addition to restricted amounts of water. During synthesis, MF is catalytically decomposed into methylamine and carbon monoxide, the former being occluded between the inorganic sheets in its protonated form.

The single-crystal structure determination shows that Mu-7 is built from zigzag aluminophosphate ladder-type chains, aluminum and phosphorus atoms being tetrahedrally coordinated to oxygens. The AlO_4 groups are 4-connected to the layers, whereas the P atoms involve one terminal oxygen atom (P═O group) and are only 3-connected to the layers. The chains are connected to form a 4 × 8 network of which Mu-7 is the first layered aluminophosphate representative. The protonated methylamine is both hydrogen bonded to the layers and neutralizes the negative charges of the anionic $[Al_3P_4O_{16}]^{3-}$ sheets.

A possible scheme of crystallization based on hydrolysis and condensation reactions of "parent" chains ($[AlP_2O_8H_2]^-$) and leading to the formation of the zigzag ladder-type chains ($[Al_4P_4O_{20}H_4]^{4-}$) is proposed. The 4 × 8 network of the new layered aluminophosphate Mu-7 could be obtained upon condensation between two zigzag ladder-type chains and one "parent" chain.

Acknowledgment. The authors thank L. Delmotte and C. Fernandez for their help.

CM991027O

(38) Kalinowski, H. O.; Berger, S.; Braun, S. In *^{13}C NMR Spektroskopie*; Verlag, G. T., Ed.; Stuttgart New York, 1984.
(39) Engelhardt, G.; Michel, D. In *High-Resolution Solid State NMR of Silicates and Zeolites*; Wiley: New Dehli, 1987.
(40) Fernandez, C.; Amoureux, J. P. *Chem. Phys. Lett.* **1995**, *242*, 449.